Int. J. Heat Mass Transfer. Vol. 34, No. 1, pp. 167–179, 1991
Printed in Great Britain

0017–9310/91 $3.00 + 0.00

Natural convection heat transfer in a partially— or completely—partitioned vertical rectangular enclosure

M. CIOFALO
Dip. di Ingegneria Nucleare, Universita di Palermo, Viale delle Scienze, Palermo, Italy

and

T. G. KARAYIANNIS
Institute of Environmental Engineering, South Bank Polytechnic, London, U.K.

(*Received* 8 *December* 1989 *and in final form* 9 *February* 1990)

Abstract—The effect of symmetric partitions protruding centrally from the end walls of a rectangular vertical enclosure on heat transfer rates is investigated numerically. The enclosure has opposite isothermal walls at different temperatures. The Rayleigh number is varied from 10^4 to 10^7 and the aspect ratio from 0.5 to 10. The thickness of the partitions is fixed and equal to one tenth of the width of the enclosure. Their non-dimensional length (L/H) is varied from 0 (non-partitioned enclosure) to 0.5 (two separate enclosures). The effect of different thermal boundary conditions at the end walls and at the partitions is included in the investigation.

INTRODUCTION

THE STUDY of heat transfer by natural convection in rectangular enclosures with differentially heated walls has been the subject of a great number of experimental and numerical investigations. This is due to their many applications such as in cavity walls, double-pane windows and solar collectors. Recently, the interests of researchers included rectangular enclosures with partial partitions, which can possibly reduce convective heat transfer rates. Nasteel and Greif [1] reported an experimental study on the effect of partial partitions extending downwards from the top end wall of a vertical enclosure of small aspect ratio, $AR = 1/2$, for $2.3 \times 10^{10} < Ra < 1.1 \times 10^{11}$. The partitions were conducting and nonconducting. They found a significant reduction in heat transfer rates across the enclosure, especially for the non-conducting partitions. In a follow-up paper the same authors [2] considered the effect of Prandtl number. They found larger heat transfer rates and a greater dependence of Nu on Ra for silicon oil than for water. They suggested that the dependence of heat transfer rates on L/H could be affected by Pr. Winters [3] examined numerically the effect of Pr in a similar geometry. He reported no significant variation in the isotherm patterns of silicon oil and water filled enclosures or in the heat transfer rates and their dependence on Ra.

In the interferometric experiments of Bajorek and Lloyd [4] the partitions were protruding into a vertical square air-filled enclosure from both the bottom and the top end walls. Their length was one quarter of the height of the enclosure. They observed a reduction in the Nusselt number along the entire hot and cold walls, and a 15% decrease in the average Nusselt number. The influence of the partitions was less pronounced at higher Grashof numbers. This is in agreement with the findings of Chang *et al.* [5] and of the present authors [6]. Chang *et al.* found that increasing the length or the thickness of the partitions resulted in larger reductions in heat transfer rates. The dependence of this reduction upon L/H was found in ref. [6] to be rather complex; short partitions ($L/H < 0.125$) can even enhance slightly the heat transfer rates across the enclosure for a certain range of AR, Ra and angle of inclination of the enclosure. In addition, Chang *et al.* reported that the efficacy of the partitions in reducing heat transfer rates may depend on the position of the partitions with respect to the hot wall.

The flow field inside partitioned and non-partitioned enclosures (similar to those studied in ref. [4]) was investigated by Bilski *et al.* [7] using laser-Doppler anemometry. Their results were compared in ref. [6] with numerical predictions and found to be in good agreement. Some disagreement was found for the peak magnitude of both horizontal and vertical velocities. Similar general good agreement, with deviations in the peak values, is also seen in the comparisons of the data of Bilski *et al.* with the numerical results of Chang *et al.* [5], Zhong *et al.* [8] and with the experimental results of Krane and Jessee [9].

ElSherbiny *et al.* [10] concluded that the thermal boundary conditions at the end walls can affect the heat transfer rates across rectangular enclosures significantly. In ref. [6] this was shown to be true both

NOMENCLATURE

AR	enclosure aspect ratio, H/W	T	dimensionless temperature, $(t-t_c)/(t_h-t_c)$
b	thickness of partitions	t_h	temperature of the hot wall
g	acceleration due to gravity	t_c	temperature of the cold wall
Gr	Grashof number, $g\beta(t_h-t_c)W^3/\nu^2$	u	velocity along x (perpendicular to isothermal walls)
H	enclosure height		
K	thermal conductivity of the fluid		
K_p	thermal conductivity of the end walls and partitions	v	velocity along y (parallel to isothermal walls)
L	partition length	U	dimensionless velocity along x, uW/α
Nu_y	local Nusselt number, $qW/(t_h-t_c)k$	V	dimensionless velocity along y, vW/α
Nu	average Nusselt number, $1/H\int_{-H/2}^{H/2} Nu_y\,dy$	x, y	coordinates (see Fig. 1)
		X, Y	dimensionless coordinates, x/W and y/W, respectively
p	pressure		
P	dimensionless pressure, $pW^2/(\rho\nu\alpha)$	W	enclosure width.
Pr	Prandtl number, ν/α		
q	local heat flux	Greek symbols	
Ra	Rayleigh number, $g\beta(t_h-t_c)W^3/\nu\alpha$	α	thermal diffusivity of the fluid
s	thickness of end walls	β	thermal expansion coefficient of the fluid
t	temperature	ν	kinematic viscosity of the fluid.

for partitioned and non-partitioned enclosures. In addition, it was verified that the thermal boundary conditions at the end walls and at the partitions' walls can influence the efficacy of the partitions in reducing heat transfer rates across the enclosure. It is expected that for both partitioned and non-partitioned enclosures the influence of the end-wall boundary conditions will decrease as the enclosure aspect ratio increases. Schinkel [11] has shown this to be true for a vertical non-partitioned enclosure at $Ra = 2\times10^5$.

MATHEMATICAL FORMULATION AND NUMERICAL METHOD

Figure 1 is a schematic of the enclosure examined in this study. The partitions protrude centrally from the top and bottom end walls. They have a finite thickness, b, which is fixed at 1/10 of the enclosure width, W.

By using dimensionless variables X, Y, U, V, P, T (defined in the Nomenclature), and the Boussinesq

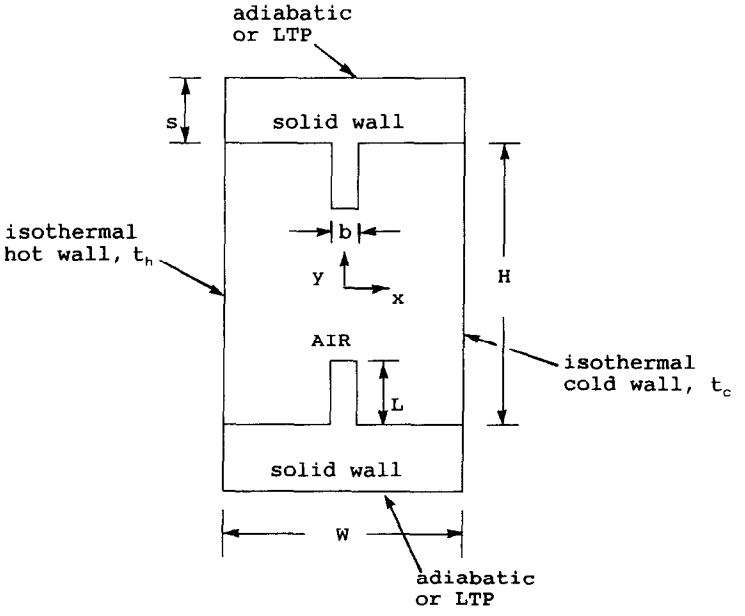

FIG. 1. Schematic of the partitioned rectangular enclosure.

approximation, the two-dimensional steady-state continuity, momentum and energy equations take the form:

$$\frac{\partial U}{\partial X}+\frac{\partial V}{\partial Y}=0 \tag{1}$$

$$\frac{1}{Pr}\left[U\frac{\partial U}{\partial X}+V\frac{\partial U}{\partial Y}\right]=-\frac{\partial P}{\partial X}+\left[\frac{\partial^2 U}{\partial X^2}+\frac{\partial^2 U}{\partial Y^2}\right] \tag{2}$$

$$\frac{1}{Pr}\left[U\frac{\partial V}{\partial X}+V\frac{\partial V}{\partial Y}\right]=-\frac{\partial P}{\partial Y}+\left[\frac{\partial^2 V}{\partial X^2}+\frac{\partial^2 V}{\partial Y^2}\right]+Ra\,T \tag{3}$$

$$U\frac{\partial T}{\partial X}+V\frac{\partial T}{\partial Y}=\frac{\partial^2 T}{\partial X^2}+\frac{\partial^2 T}{\partial Y^2}. \tag{4}$$

The flow boundary conditions were:

$$U=V=0 \text{ on solid boundaries.} \tag{5}$$

The thermal boundary conditions on the isothermal walls were:

$$T=1 \text{ at } X=-1/2 \text{ (hot wall)}$$

$$T=0 \text{ at } X=1/2 \text{ (cold wall).} \tag{6}$$

At the end walls and the partitions different sets of thermal boundary conditions were considered. They are sketched in Fig. 2 and will be discussed in detail in the following section.

In this study, Ra was varied between 10^4 and 10^7, AR between 0.5 and 10, and L/H between 0 (non-partitioned enclosure) and 0.5 (two separate enclosures). Equations (1)–(4) above were solved using the computer code Harwell-FLOW3D [12], which is based on a finite-difference, centred-grid, method. The SIMPLEC algorithm for pressure–velocity coupling was chosen [13]. The convergence criterion to stop the outer iterations was that the mass flow residual fell below 10^{-3} times the mass flow associated with the main circulation cell. Non-uniform computational grids, having 24×24 control volumes in the case of non-partitioned enclosures, and 32×32 in the case of partitioned enclosures, were adopted (Figs. 3(a) and (b)). This allowed satisfactory grid-independence of the most relevant computational result (average Nusselt number, Nu), as shown in Fig. 4 for the case $AR=10$, $L/H=0$ and 0.25, $Ra=3.5\times10^5$, and adiabatic thermal boundary conditions. Additional control volumes were used in the end walls in the case of 'generalized' boundary conditions (Figs. 2(iii) and (iv)). The central differencing scheme (CDS) was used whenever possible for the advective terms in order to prevent numerical diffusion errors. Up to $Ra=3.5\times10^5$ results obtained by using CDS and hybrid-upwind differencing (HDS) differed less than 1% in Nu and negligibly in the peak velocities. For $Ra=1\times10^6$ and 3.5×10^6 the CDS solution exhibited some spurious oscillations and convergence was achieved only by using small underrelaxation factors, while the difference in Nu between the CDS and the HDS results increased to 3% in the worst case

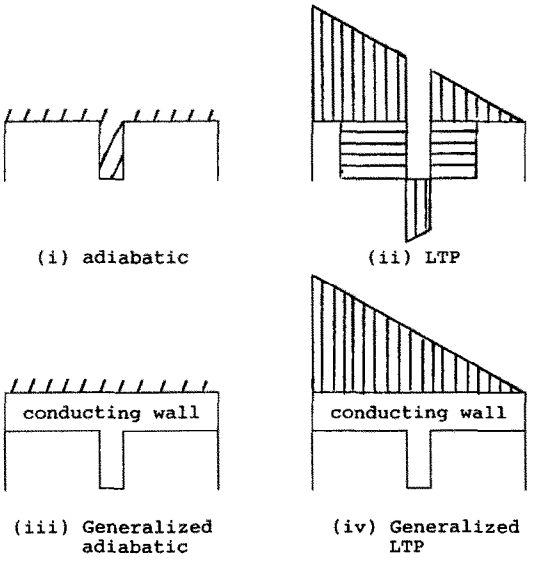

FIG. 2. Thermal boundary conditions at the end walls and partitions.

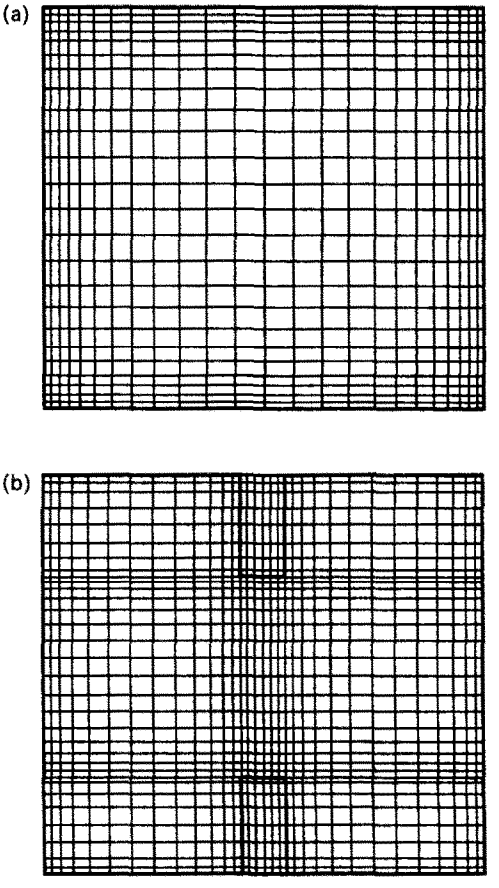

FIG. 3. Computational grids for a non-partitioned and for a partitioned enclosure (fluid region only): (a) non-partitioned enclosure (24×24); (b) partitioned enclosure, $L/H=0.25$ (32×32).

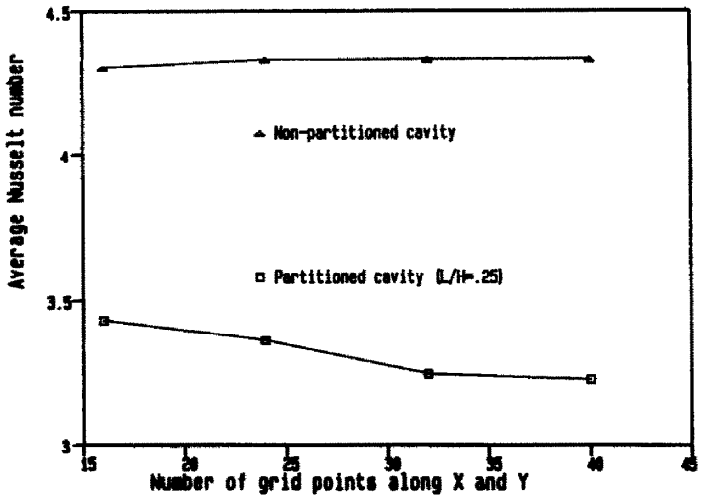

FIG. 4. Sensitivity of Nu to the number of grid points for a partitioned and a non-partitioned enclosure ($Ra = 3.5 \times 10^5$, $AR = 10$, adiabatic boundary conditions).

($AR = 10$, $L/H = 0$, LTP, 24×24 grid). For $Ra = 1 \times 10^7$ convergence was obtained only with HDS. All results presented here are based on HDS only at the highest Rayleigh number (1×10^7) and on CDS otherwise. Computation times, ranged from 1 to 20 s on an IBM 3090, depending on Rayleigh number, partition length, aspect ratio and boundary conditions.

EFFECT OF THERMAL BOUNDARY CONDITION ON HEAT TRANSFER RATES

Non-partitioned enclosures

For non-partitioned enclosures ($L/H = 0$) the following end-wall thermal boundary conditions were tested:

(i) adiabatic: $\partial T/\partial Y = 0$;

(ii) linear temperature profile (LTP): $T = 1/2 - X$;

(iii) generalized adiabatic: end walls of finite thickness, s, and conductivity, K_p, with $\partial T/\partial Y = 0$ along their outer sides;

(iv) generalized LTP: as in (iii) above, but with $T = 1/2 - X$ along their outer sides.

When the 'generalized' boundary conditions (iii) or (iv) are used, the ratios s/W and K_p/K become important parameters. For generalized adiabatic conditions, it was shown in ref. [6] that varying s/W and K_p/K results in a variation of the local and average Nusselt number between the maximum and minimum values that are obtained with adiabatic (i) and (ii) conditions, respectively. Results obtained for a square vertical non-partitioned cavity at $Ra = 3.5 \times 10^5$ are summarized in Fig. 5(a); it shows Nu isopleths in the plane of s/W and K_p/K. As seen in the figure, Nu reaches an asymptotic value for $K_p/K > 10$ at all values of s/W, and for $s/W > 1$ at all values of K_p/K.

In the present study, the effect of varying s/W and K_p/K for the 'generalized LTP' case was also investigated. Results are more complex than for the 'generalized adiabatic' case; they are summarized in Fig. 5(b), again for a vertical non-partitioned enclosure at $Ra = 3.5 \times 10^5$. The maximum value of Nu, 6.6, can be obtained for a large range of s/W and small K_p/K. Similarly, the minimum value, 4.9, can be obtained for a large range of K_p/K and small s/W. (Note that with 'generalized adiabatic' boundary conditions the minimum Nu of 4.9, corresponding to LTP boundary conditions (ii), cannot be attained for any combination of s/W and K_p/K.)

In all subsequent runs, and in accordance with earlier work of the present authors, the values $s/W = 0.1$ and $K_p/K = 100$ were chosen as representative of realistic configurations and used in conjunction with 'generalized adiabatic' and 'generalized LTP' conditions. The resulting set of boundary conditions will be referred to as 'standard adiabatic' and 'standard LTP' throughout this paper.

An impression of the influence of thermal boundary conditions on heat transfer rates is given by Fig. 6, which reports Nu as a function of Ra for a non-partitioned square enclosure ($AR = 1$) under all four boundary conditions. Several experimental and numerical results by different authors are reported for comparison. Our results are in excellent agreement with the numerical predictions of Schinkel [11], Catton *et al.* [14] and Chen and Talaie [15], who assumed either adiabatic or LTP end walls. The agreement with the experimental results of Bajorek and Lloyd [4] and Schinkel [11] is best when LTP conditions are assumed. Some disagreement exists with the experimental results of Arnold *et al.* [16] especially at high Rayleigh numbers.

Figure 7 reports similar comparisons for an enclosure having $AR = 10$. The experimental results of ElSherbiny [17] fall slightly above the present predictions, while the predictions of Chen and Talaie [15]

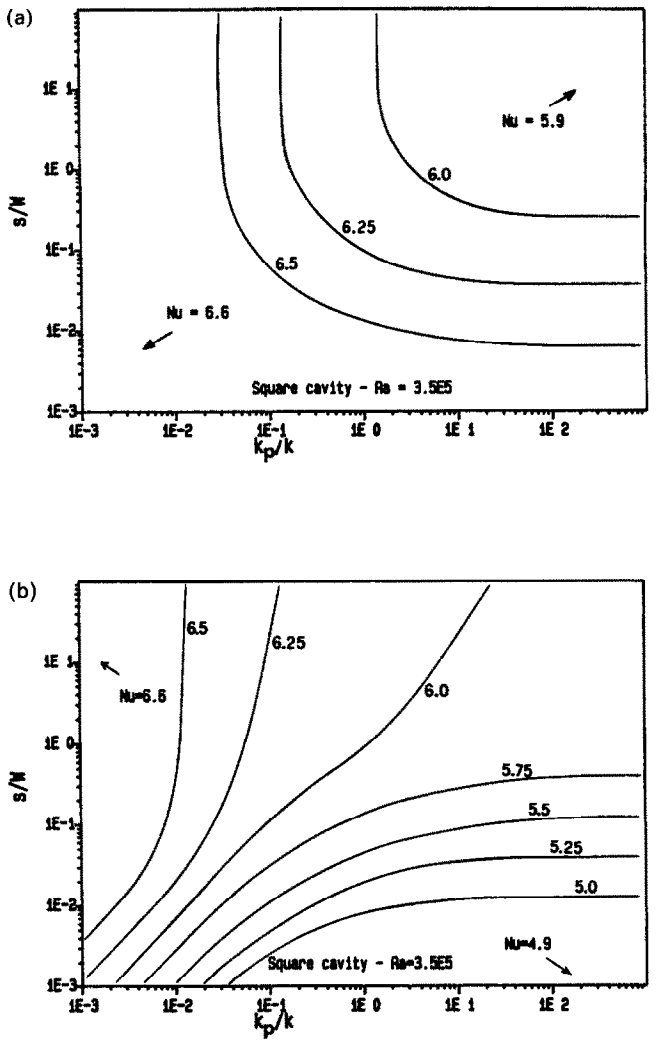

FIG. 5. Dependence of Nu upon s/W and k_p/k for a square, non-partitioned enclosure at $Ra = 3.5 \times 10^5$ when 'generalized' boundary conditions are used: (a) 'generalized adiabatic' boundary conditions; (b) 'generalized LTP' boundary conditions.

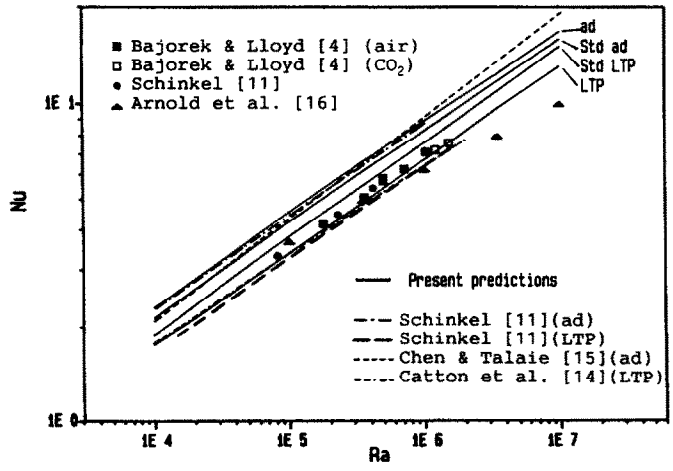

FIG. 6. Comparison of results for $AR = 1$, non-partitioned enclosure (lines, predictions; symbols, experimental data).

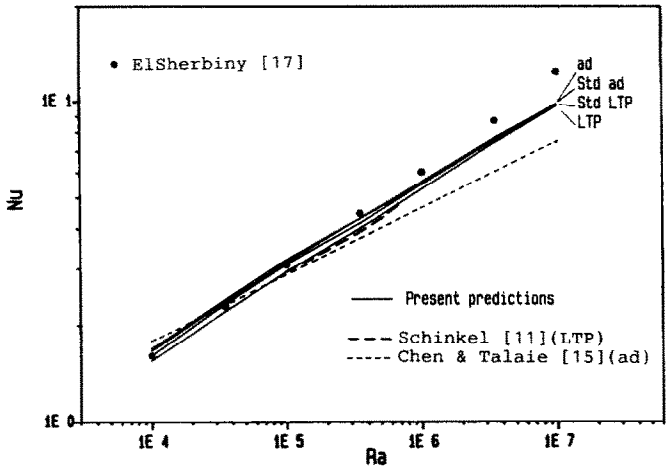

FIG. 7. Comparison of results for $AR = 10$, non-partitioned enclosure (lines, predictions; symbols, experimental data).

fall below them. The difference in Nu associated with the use of different boundary conditions is smaller than for $AR = 1$, but is still significant, especially at low Rayleigh numbers.

The dependence of Nu upon Ra can be approximated for all aspect ratios by

$$Nu = 1 \qquad (Ra < 10^3)$$
$$Nu = f(AR) \cdot Ra^{1/4} \qquad (Ra > 10^4) \qquad (7)$$

with a smooth fit between the two regions. The exponent of Ra is slightly larger than 1/4 (0.27–0.28) for the lower aspect ratios (0.5, 1). The function f is different for each set of boundary conditions. The local Nusselt number, Nu_y, along the hot wall, computed using all four boundary conditions, for a square non-partitioned enclosure at $Ra = 3.5 \times 10^5$, is compared with experimental results of Bajorek and Lloyd [4] in Fig. 8(a). 'Standard LTP' conditions give the best agreement (see also the reported values of Nu). Clearly, they approximate better than the others the actual thermal boundary conditions of the experiments (see discussion in refs. [6, 18]).

EFFECT OF THERMAL BOUNDARY CONDITIONS ON HEAT TRANSFER RATE

Partitioned enclosures

In the case of partitioned enclosures, the thermal boundary conditions at the partitions' walls also play a role. Partitions can be assumed to be adiabatic, isothermal, or conducting, and their thickness and conductivity must be considered. By combining these options with those concerning the end walls, a very large number of possible boundary conditions ensues. However, in the present study the following simplifying assumptions were made (see Fig. 2). The most natural extension of adiabatic conditions consists of assuming the partitions to be also adiabatic. LTP conditions can be extended to partitioned enclosures assuming the partitions' walls to be isothermal (at $T = 0.5$ for infinitely thin partitions, or at the appropriate corner temperature along end walls in the case of finite-thickness partitions). Finally, 'generalized' conditions can be extended by assuming conducting partitions, having the same K_p/K ratio as the end walls.

In Fig. 8(b), the local Nusselt number computed using the boundary conditions defined above is compared with experimental results of ref. [4] for a square enclosure having $L/H = 0.25$ at $Ra = 3.5 \times 10^5$. The experimental points lie closest to the LTP predictions (see also reported values of Nu). Thus, both for partitioned and non-partitioned enclosures LTP or 'standard LTP' boundary conditions yield better agreement with the experimental results of Bajorek and Lloyd than adiabatic or 'standard adiabatic' ones.

The influence of boundary conditions on heat transfer rates for different partition lengths can be observed in Fig. 9, which reports Nu as a function of L/H for $Ra = 3.5 \times 10^5$, $AR = 1$ and all four boundary conditions. For short partitions, adiabatic conditions still give the highest value of Nu, and LTP conditions the lowest. However, for long partitions, adiabatic conditions yield low heat transfer rates, as Nu tends to zero in the limit of $L/H \to 0.5$. The value of L/H at which the adiabatic curve falls below the others is ~ 0.4 for this AR and Ra. Our results show that this value increases with Ra and with AR.

For both partitioned and non-partitioned enclosures, the influence of thermal boundary conditions decreases with increasing aspect ratio. This is shown in Fig. 10, which reports the percentage difference between adiabatic and LTP predictions as a function of AR for $Ra = 3.5 \times 10^5$ and $L/H = 0$, 0.125, and 0.25. As seen in the figure, the influence of boundary conditions is higher for partitioned than for non-partitioned enclosures.

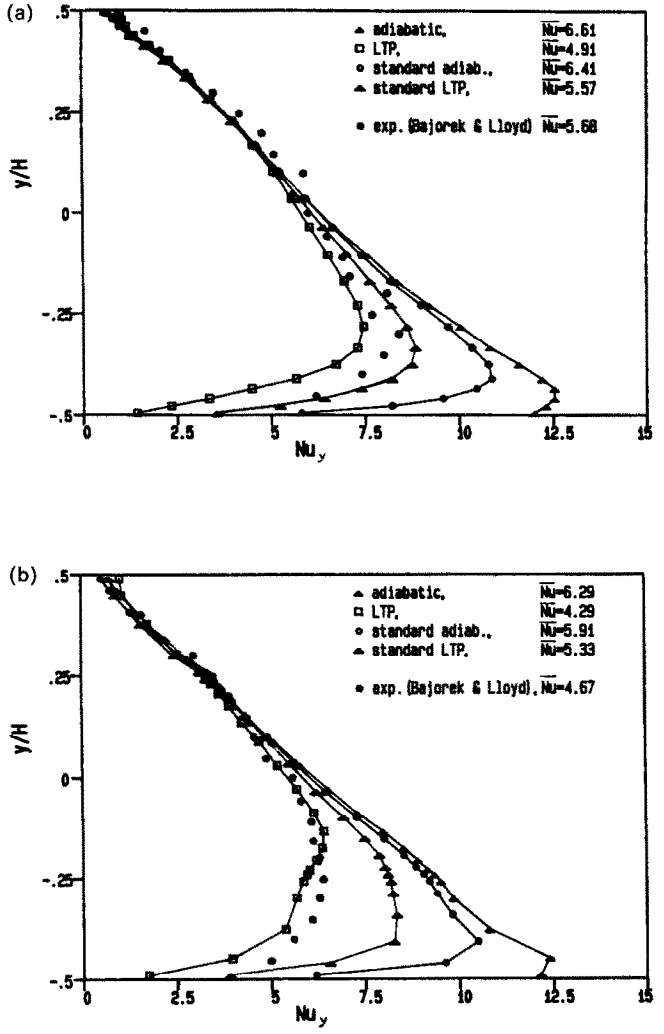

FIG. 8. Nusselt number profiles along the hot wall for a non-partitioned and a partitioned enclosure (experimental data [4] vs predictions using different thermal boundary conditions): (a) non-partitioned enclosure, $AR = 1$, $Ra = 3.5 \times 10^5$; (b) partitioned enclosure, $AR = 1$, $Ra = 3.5 \times 10^5$.

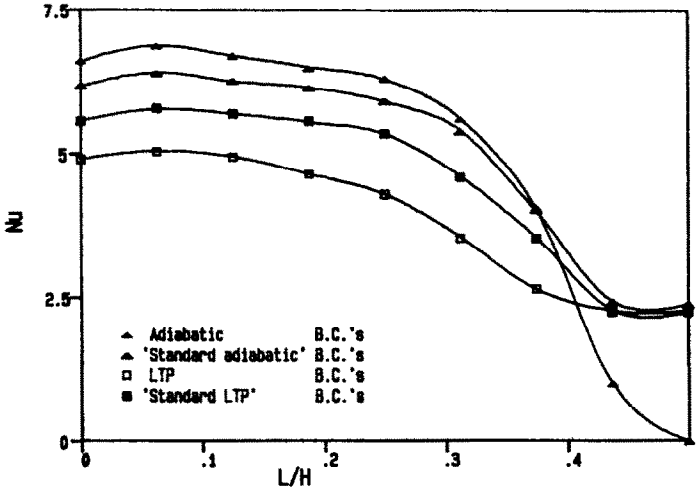

FIG. 9. Dependence of Nu on the partition length for different thermal boundary conditions ($AR = 1$, $Ra = 3.5 \times 10^5$).

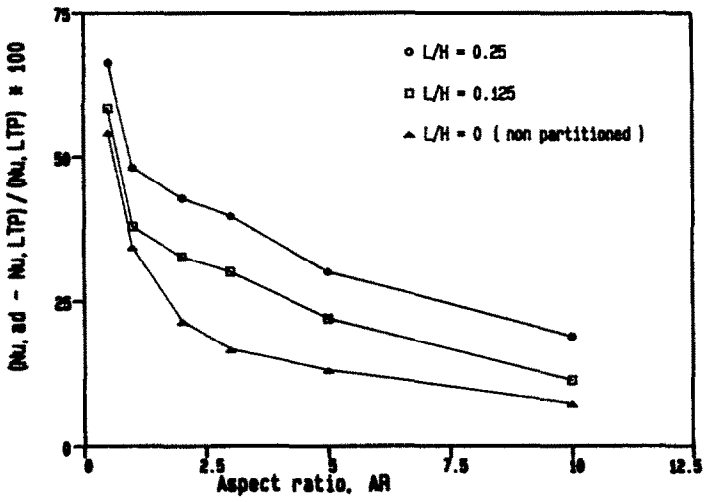

FIG. 10. Percentage difference between values of Nu computed using adiabatic and LTP boundary conditions as a function of the aspect ratio ($Ra = 3.5 \times 10^5$).

EFFECT OF PARTITIONS ON HEAT TRANSFER RATES

Figure 9 shows that, under the conditions considered ($AR = 1$, $Ra = 3.5 \times 10^5$), short partitions ($L/H < 0.125$) do *not* reduce Nu. In fact, they may enhance slightly the heat transfer rate. In our computations, this was found to occur at $AR = 1$ and 2 and Ra in the range 10^5–10^6.

Figures 11 and 12 are plots of Nu vs Ra for $AR = 1$ and 10, respectively, and for different values of L/H including the case of two separate coupled enclosures ($L/H = 0.5$). Examination of these figures shows that, for a given aspect ratio, the effect of partitions is much more pronounced at lower Rayleigh numbers. This is in agreement with refs. [4, 5] and with earlier work of the present authors [6]. For LTP conditions (Figs. 11(b) and 12(b)), it can be observed that an enclosure having long partitions ($L/H = 0.375$) behaves much like a completely divided enclosure at low Ra, but much like a non-partitioned enclosure at high Ra. By comparing Figs. 11 and 12, it can be seen that short partitions ($L/H < 0.25$) are much more effective at high aspect ratios. The influence of AR on the efficacy of partitions is better evidenced in Fig. 13 which shows Nu as a function of AR at $Ra = 3.5 \times 10^5$ for different values of L/H and for adiabatic and LTP boundary conditions. Short partitions are least effective at $1 \leqslant AR \leqslant 3$. Thus, the case of the square cavity is *not* representative in this respect.

The present investigation showed two basic mechanisms by which partitions can reduce heat transfer rates in enclosures. At low aspect ratios, partitions do not alter the unicellular flow pattern, typical of the non-partitioned enclosure. Thus, their effect is limited to reducing the fluid flow rate along the isothermal walls, thus reducing moderately, and more or less uniformly, the local Nusselt number. This is shown in Figs. 14(a)–(c) for $Ra = 3.5 \times 10^5$ and $AR = 1$. Only LTP results are reported. They include profiles of Nu_y along the hot wall for different L/H (a), plus streamlines (b) and isotherms (c) for $L/H = 0.25$. The reduction in Nu for this value of L/H is only 12%; the corresponding reduction in the flow rate is $\sim 25\%$.

At high aspect ratios, on the contrary, the presence of partitions results in the breaking down of the unicell, and in the formation of secondary cells particularly intense near the bottom of the hot wall and the top of the cold wall (i.e. where Nu has a maximum in the non-partitioned enclosure). This results in a strong local reduction of Nu_y; the enclosure behaves much like a stack of three cavities, the central one being scarcely affected by the partitions and the extreme ones being almost completely divided. Also the average Nusselt number decreases more than in the low-aspect ratio case. This is shown in Figs. 15(a)–(c) for $AR = 10$, $Ra = 3.5 \times 10^5$, LTP boundary conditions. The $L/H = 0.25$ partitions reduce Nu by 30% in this case, while the corresponding reduction in the mass flow rate is 31%.

The case $L/H = 0.5$ (complete partition dividing the enclosure in two separate zones) has been particularly studied, both experimentally and numerically for its special relevance to engineering applications such as multiple-glazed solar collectors or windows. Anderson and Bejan [19] reported that a thin central aluminium partition in a water-filled enclosure having $AR = 1/3$ at $Ra = 10^9$–10^{11} reduced the overall heat transfer rate by a factor $(N+1)^{-0.61}$ where N is the number of partitions (a factor of 0.66 for $N = 1$). Nishimura *et al.* [20] performed both an experimental and a numerical investigation. In their experiments the partitions were made of thin copper plates. The working fluid was water, the enclosure aspect ratios were 4 and 10 and $10^6 \leqslant Ra \leqslant 10^9$. In these experiments they found a heat transfer reduction by a factor of 0.42 for a single partition. In their numerical simu-

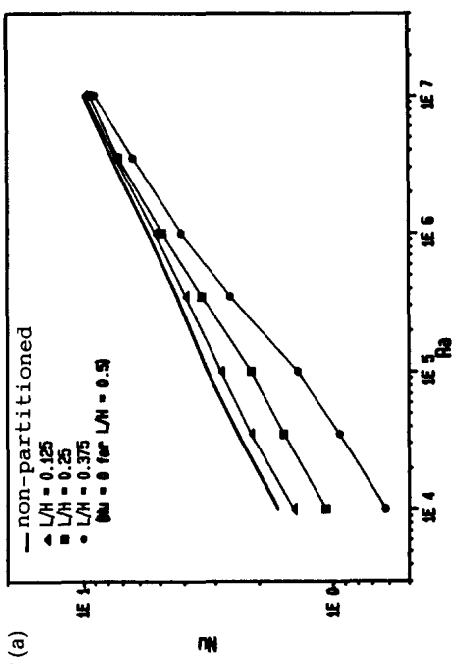

FIG. 11. *Nu* vs *Ra* for $AR = 1$ and different partition lengths: (a) adiabatic boundary conditions; (b) LTP boundary conditions.

FIG. 12. *Nu* vs *Ra* for $AR = 10$ and different partition lengths: (a) adiabatic boundary conditions; (b) LTP boundary conditions.

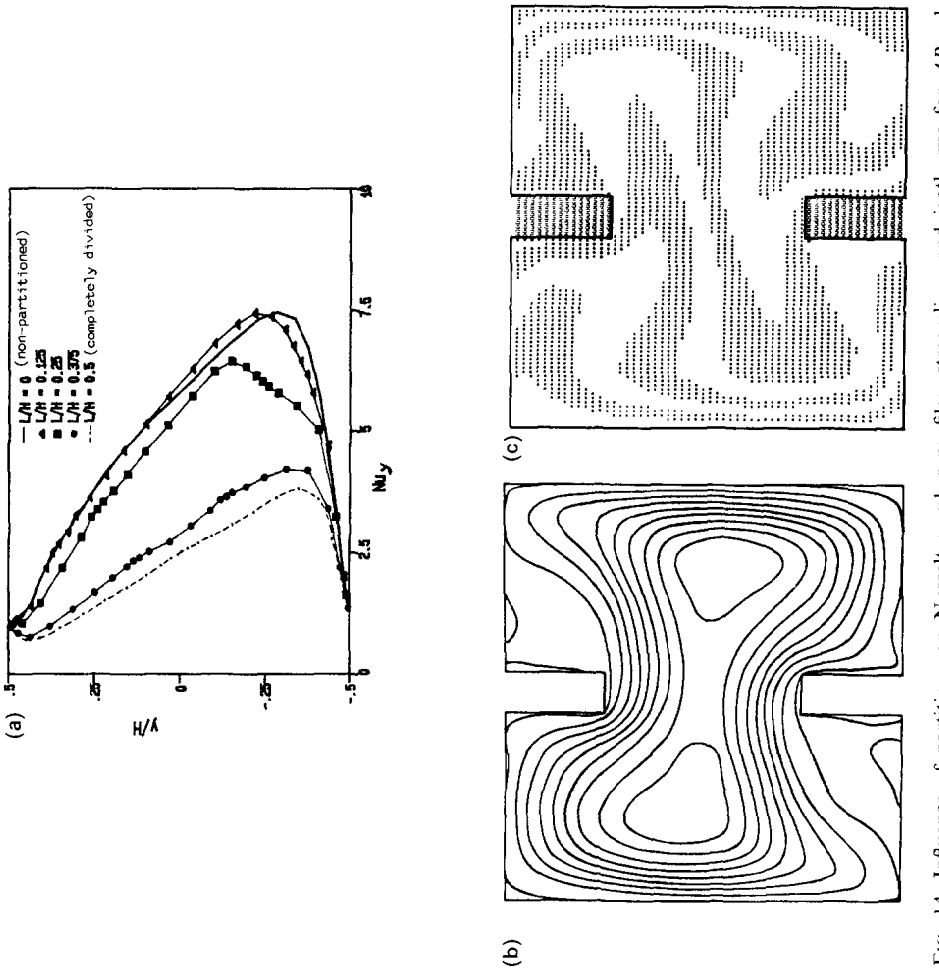

FIG. 14. Influence of partitions on Nusselt number profiles, streamlines and isotherms for $AR = 1$, $Ra = 3.5 \times 10^5$ and LTP boundary conditions: (a) Nusselt number profiles along the hot wall for different values of L/H; (b) streamlines for $L/H = 0.25$; (c) isotherms for $L/H = 0.25$.

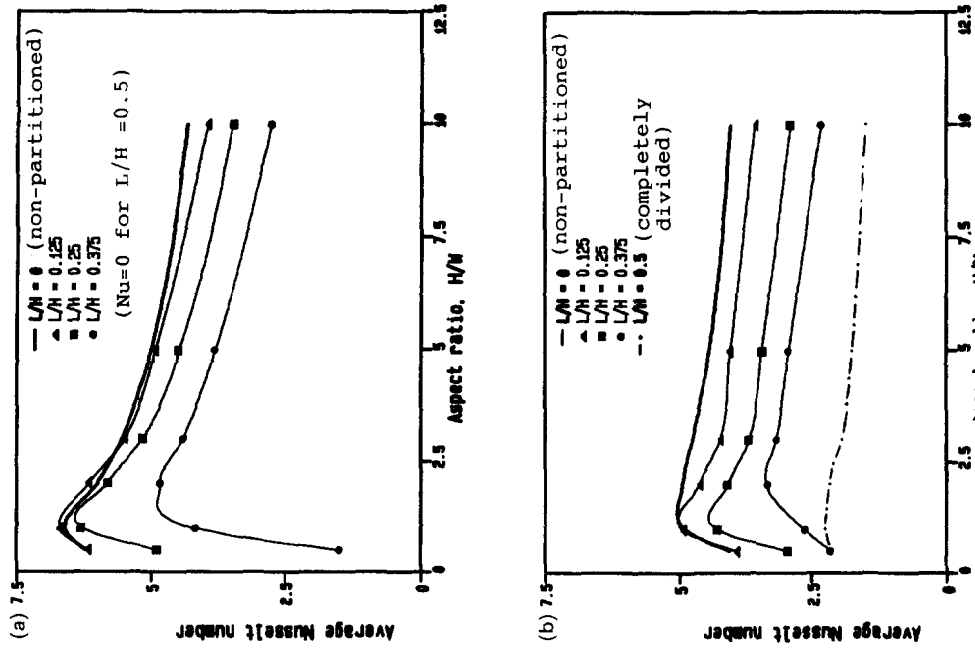

FIG. 13. Nu vs AR for different values of L/H ($Ra = 3.5 \times 10^5$): (a) adiabatic boundary conditions; (b) LTP boundary conditions.

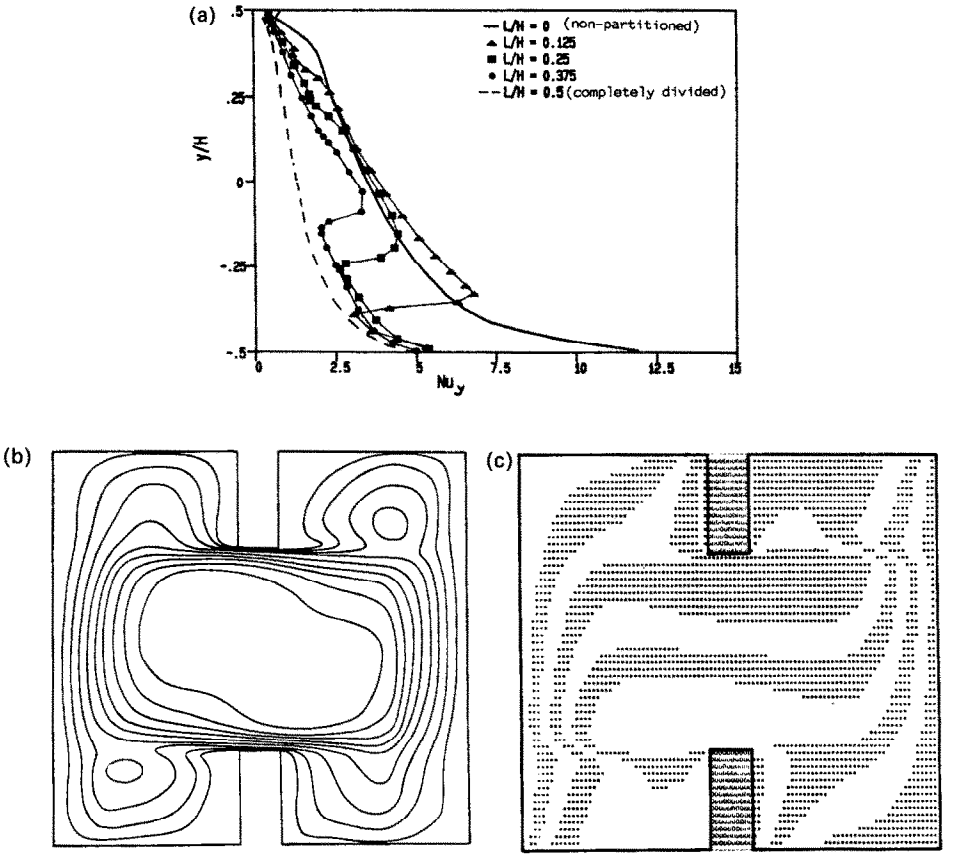

FIG. 15. Influence of partitions on Nusselt number profiles, streamlines and isotherms for $AR = 10$, $Ra = 3.5 \times 10^5$ and LTP boundary conditions: (a) Nusselt number profiles along the hot wall for different values of L/H; (b) streamlines for $L/H = 0.25$; (c) isotherms for $L/H = 0.25$.

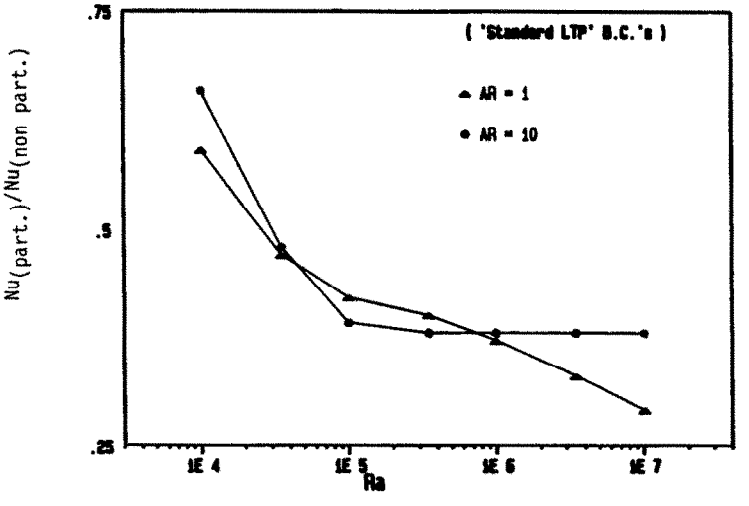

FIG. 16. Reduction in Nu induced by a complete partition ($L/H = 0.5$) for $AR = 1$ and 10.

lations ($AR = 4$, $Pr = 6$, $10^4 \leqslant Ra \leqslant 10^7$) they reported a reduction by a factor $(N+1)^{-1}$ (a factor of 0.5 for $N = 1$).

A simplified analysis reveals that, if the central partition is assumed to be infinitely thin and isothermal (at $T = 1/2$), its effect consists merely of replacing the original enclosure (having aspect ratio AR and Rayleigh number Ra) with two enclosures in series, each having an aspect ratio $2AR$ and Rayleigh number $Ra/16$. Thus, if the dependence of Nu upon AR and

Ra is generically indicated as $Nu = g(AR, Ra)$, the expected reduction factor due to the partition is

$$Nu_{\text{part}}/Nu_{\text{non-part}} = g(2AR, Ra/16)/g(AR, Ra). \quad (8)$$

In the limit of high AR and high Ra, but still in the laminar region, Nu becomes roughly independent of AR and increases as $Ra^{1/4}$, so that the expected reduction factor is $(1/16)^{1/4} = 0.5$. For low AR, a smaller reduction factor is expected, due to Nu decreasing with increasing AR (Fig. 13). For low Ra ($< 1 \times 10^4$), the reduction factor will be larger, due to Nu tending to 1 for $Ra \to 0$ (equation (7)). Deviations from this overall behaviour will result from the thermal coupling [21, 22] in this case between the two demi-enclosures across a conducting partition, and from the finite thickness of the partition.

Among the present computational results for $L/H = 0.5$, the 'standard adiabatic' and 'standard LTP' ones, in which both the end walls and the partitions are assumed to be of finite thickness $0.1W$ and conductivity $100K$, are closest to situations of practical interest. Note, however, that Fig. 9 shows the resulting Nu at $L/H = 0.5$ to be almost coincident with that computed under LTP conditions (roughly corresponding to an isothermal partition at $T = 1/2$). This indicates that the effect of the thermal coupling between the two demi-enclosures is not very large. The reduction factor predicted with 'standard LTP' boundary conditions is reported as a function of Ra in Fig. 16 for $AR = 1$ and 10. The results are coherent with the above analysis from a qualitative point of view. The issue of coupled flows in completely partitioned enclosures, however, requires further and more detailed investigation.

CONCLUSIONS

A parametrical study was conducted on the efficacy of partitions, protruding from the end walls of a vertical rectangular enclosure, in reducing heat transfer rates. Over 400 cases, covering the range $AR = 0.5$–10, $Ra = 10^4$–10^7, and $L/H = 0$–0.5, were computed. The influence of thermal boundary conditions at the end walls and at the partitions was studied and found to be relevant, specially for low-aspect ratio enclosures. 'Generalized' boundary conditions were introduced as more appropriate to simulate situations of practical engineering interest. The efficacy of the partitions was found to depend in a complex way upon AR and Ra, and to be greatest for low Ra and high AR. The mechanism responsible for this large reduction in heat transfer rates was found to be the breaking down of the unicellular circulation near the regions where Nu_y is maximum in non-partitioned enclosures. However, partitions having $L/H < 0.25$ never reduce Nu by more than 30%. For intermediate AR (1–2) and Ra (10^5–10^6), very short partitions are not effective and can even enhance heat transfer rates. For completely divided enclosures ($L/H = 0.5$) our results indicate a reduction in Nu by a factor ~ 0.4 for $AR = 10$ and high Ra ($Ra > 10^5$), while no simple scaling law is applicable for small aspect ratio and Ra.

REFERENCES

1. M. W. Nasteel and R. Greif, Natural convection in undivided and partially divided rectangular enclosures, *ASME J. Heat Transfer* **103**, 623–629 (1981).
2. M. W. Nasteel and R. Greif, Natural convection heat transfer in complex enclosures at large Prandtl number, *ASME J. Heat Transfer* **105**, 912–915 (1983).
3. K. H. Winters, Laminar natural convection in a partially divided rectangular cavity at high Rayleigh number, *Int. J. Numer. Meth. Fluids* **8**, 247–281 (1988).
4. S. M. Bajorek and J. R. Lloyd, Experimental investigation of natural convection in partitioned enclosures, *ASME J. Heat Transfer* **104**, 527–532 (1982).
5. L. C. Chang, J. R. Lloyd and K. T. Yang, A finite difference study of natural convection in complex enclosures, *Proc. 7th Int. Heat Transfer Conf.*, Munich, pp. 183–188 (1982).
6. M. Ciofalo and T. G. Karayiannis, Natural convection in a rectangular partitioned cavity, *Proc. 7th Natn. Conf. of the UIT (Unione Italiana di Termofluidodinamica)*, Florence, Italy, pp. 31–55 (1989).
7. S. M. Bilski, J. R. Lloyd and K. T. Yang, An experimental investigation of the laminar natural convection velocity field in square and partitioned enclosures, *Proc. 8th Int. Heat Transfer Conf.*, San Francisco, Vol. 4, pp. 1513-1518 (1986).
8. Z. Y. Zhong, K. T. Yang and J. R. Lloyd, Variable property effects in laminar natural convection in a square cavity. In *ASME Natural Convection in Enclosures* (Edited by I. Catlin and K. E. Torrance), Vol. 26, pp. 69–75 (1983).
9. R. J. Krane and J. Jessee, Some detailed field measurements for natural convection flow in a vertical square enclosure, *Proc. ASME–JSME Thermal Engng Joint Conf.*, Hawaii, pp. 323–329 (1983).
10. S. M. ElSherbiny, K. G. T. Holland and G. T. Raithby, Effect of the thermal boundary condition on natural convection in vertical and inclined air layers, *Proc. 20th ASME–AIChE Natn. Heat Transfer Conf.*, Milwaukee, Wisconsin, HT Vol. 16, pp. 127–133 (1981).
11. W. M. M. Schinkel, Natural convection in inclined air-filled enclosures, Dutch Efficiency Bureau, Pijnacker (1980).
12. A. D. Burns, I. P. Jones, J. R. Kightley and N. S. Wilkes, Harwell–FLOW3D Release 2.1—User Manual, UKAEA Report AERE-R (Draft) (August 1988).
13. J. P. Van Doormal and G. D. Raithby, Enhancement of the SIMPLE method for predicting incompressible fluid flows, *Numer. Heat Transfer* **7**, 147–163 (1984).
14. I. Catton, P. S. Ayyaswamy and R. N. Clever, Natural convection flow in a finite rectangular slot arbitrarily oriented with respect to the gravity vector, *Int. J. Heat Mass Transfer* **17**, 173–184 (1974).
15. C. J. Chen and V. Talaie, Finite analytical numerical solutions of laminar natural convection in two-dimensional inclined rectangular enclosures, ASME Paper 85-HT-10 (1985).
16. J. N. Arnold, I. Catton and D. K. Edwards, Experimental investigation of natural convection in inclined rectangular regions of different aspect ratios, *ASME J. Heat Transfer* **98**, 67–71 (February 1976).
17. S. M. ElSherbiny, Heat transfer by natural convection across vertical and inclined air layers, Ph.D. Thesis, University of Waterloo, Ontario, Canada (1980).
18. M. Ciofalo and T. G. Karayiannis, Convective heat

transfer in a vertical square cavity with partitions at the end walls, Eurotherm Seminar No. 11, Natural Convection in Enclosures, Harwell, U.K., 7–8 December (1989).
19. R. Anderson and A. Bejan, Heat transfer through single and double vertical walls in natural convection—theory and experiment, *Int. J. Heat Mass Transfer* **24,** 1611–1620 (1981).
20. T. Nishimura, M. Shiraishi, F. Nagasawa and Y. Kawamura, Natural convection heat transfer in enclosures with multiple vertical partitions, *Int. J. Heat Mass Transfer* **31,** 1679–1686 (1988).
21. E. M. Sparrow and C. Prakash, Interaction between internal natural convection in an enclosure and an external natural convection boundary layer flow, *Int. J. Heat Mass Transfer* **24,** 895–903 (1981).
22. T. G. Karayiannis and J. D. Tarasuk, Natural convection in an inclined rectangular cavity with different thermal boundary conditions at the top plate, *ASME J. Heat Transfer* **110,** 350–357 (1988).

CONVECTION THERMIQUE NATURELLE DANS UNE CAVITE RECTANGULAIRE VERTICALE PARTIELLEMENT OU COMPLETEMENT CLOISONNEE

Résumé—On étudie numériquement l'effet sur les flux thermiques de partitions symétriques partant du centre des parois terminales d'une cavité rectangulaire verticale. La cavité a des parois opposées isothermes à des températures différentes. Le nombre de Rayleigh varie de 10^4 à 10^7 et le rapport de forme de 0,5 à 10. L'épaisseur des cloisons est fixée égale à un dixième de la largeur de la cavité. Leur longueur adimensionnelle (L/H) varie de zéro (cavité sans cloison) à 0,5 (deux cavités séparées). On considère dans l'étude l'effet de différentes conditions aux limites sur les parois terminales et sur les cloisons.

NATÜRLICHE KONVEKTION IN EINEM TEILWEISE—ODER VOLLSTÄNDIG—UNTERTEILTEN SENKRECHTEN RECHTWINKLIGEN HOHLRAUM

Zusammenfassung—Der Einfluß symmetrischer Trennwände, die in einem rechtwinkligen vertikalen Hohlraum in der Mitte der Stirnwände herausstehen, auf den Wärmeübergangskoeffizienten wird numerisch untersucht. Der Hohlraum besitzt gegenüberliegende isotherme Wände mit unterschiedlichen Temperaturen. Die Rayleigh-Zahl wird von 10^4 bis 10^7 und das Seitenverhältnis von 0,5 bis 10 variiert. Die Dicke der Trennwände ist unveränderlich. Sie entspricht einem Zehntel der Hohlraumbreite. Ihre dimensionslose Länge (L/H) wird von 0 (nicht unterteilter Hohlraum) bis 0,5 (zwei getrennte Hohlräume) variiert. Die Auswirkung unterschiedlicher thermischer Randbedingungen an den Stirnseiten und an den Trennwänden wird in die Untersuchung einbezogen.

ЕСТЕСТВЕННОКОНВЕКТИВНЫЙ ТЕПЛОПЕРЕНОС В ЧАСТИЧНО ИЛИ ПОЛНОСТЬЮ СЕКЦИОНИРОВАННЫХ ВЕРТИКАЛЬНЫХ ПРЯМОУГОЛЬНЫХ ПОЛОСТЯХ

Аннотация—Численно исследуется влияние симметричных перегородок, установленных в центральной части торцевых границ вертикальной полости, на интенсивность теплопереноса. На противоположных изотермических стенках полости поддерживаются различные температуры. Значения числа Рэлея изменяются в диапазоне 10^4–10^7, а отношение размеров полости (H/W) от 0,5 до 10. Толщина перегородок постоянна и составляет одну десятую часть от ширины полости. Их безразмерная длина (L/H) изменяется от нуля (несекционированная полость) до 0,5 (две раздельные полости). Исследовалось влияние различных тепловых условий на торцевых границах и перегородках на интенсивность теплопереноса.